HHS Public Access

Author manuscript

Biol Psychiatry. Author manuscript; available in PMC 2017 October 01.

Published in final edited form as:

Biol Psychiatry. 2016 October 01; 80(7): 509–521. doi:10.1016/j.biopsych.2016.05.012.

Circuit based cortico-striatal homologies between rat and primate

Sarah R. Heilbronner, PhD[1], **Jose Rodriguez-Romaguera, PhD**[2], **Gregory J. Quirk, PhD**[2], **Henk J. Groenewegen, PhD**[3], and **Suzanne N. Haber, PhD**[1]

[1]Department of Pharmacology and Physiology, University of Rochester Medical Center, Rochester, NY 14642 [2]Departments of Psychiatry and Anatomy & Neurobiology University of Puerto Rico School of Medicine, San Juan, PR 00936 [3]Department of Anatomy and Neurosciences, Neuroscience Campus Amsterdam, VU University Medical Center, 1007 MB Amsterdam, The Netherlands

Abstract

BACKGROUND—Understanding the neural mechanisms of psychiatric disorders requires the use of rodent models; however, frontal-striatal homologies between rodents and primates are unclear. In contrast, within the striatum, the shell of the nucleus accumbens, the hippocampal projection zone, and the amygdala projection zone (referred to as the striatal emotion processing network, EPN) are conserved across species. We used the relationship between the EPN and projections from the anterior cingulate and orbitofrontal cortices (ACC/OFC) to assess network similarities across rats and monkeys.

METHODS—We first compared the location and extent of each major component of the EPN in rats and macaques. Next, we used anatomical cases with anterograde injections in ACC/OFC to determine the extent to which cortico-striatal terminal fields overlapped with these components, and with each other.

RESULTS—The location and size of each component of the EPN were similar across species, containing projections primarily from infralimbic cortex (IL) in rats and area 25 (a25) in monkeys. Other ACC/OFC terminals overlapped extensively with IL/a25 projections, supporting cross-species similarities between medial versus lateral OFC. However, dorsal ACC had different connectivity profiles across species. These results were used to segment the monkey and rat striata according to ACC/OFC inputs.

CONCLUSIONS—Based on connectivity with the EPN, and consistent with prior literature, IL and a25 are likely homologues. We also see evidence of homologies across medial versus lateral

Address for Correspondence: Suzanne N. Haber, PhD, University of Rochester Medical Center, School of Medicine and Dentistry, 601 Elmwood Ave, Box 711, Rochester, NY 14642, Phone: 585-275-4538, Fax: 585-273-2652, suzanne_haber@urmc.rochester.edu.

Financial Disclosures

The authors report no biomedical financial interests or potential conflicts of interest.

OFC. Along with segmenting the striatum and identifying striatal hubs of overlapping inputs, these results help to translate findings between rodent models and human pathology.

Keywords

orbitofrontal; prefrontal; cingulate; prelimbic; infralimbic; homology

Introduction

Abnormalities of anterior cingulate (ACC)- and orbitofrontal (OFC)-striatal circuits are at the root of several psychiatric disorders, including post-traumatic stress disorder (PTSD), obsessive-compulsive disorder (OCD), addiction, and major depressive disorder (MDD) (1–4). While studies in humans highlight the association between these circuits and disease, research on rodents is essential for understanding the mechanisms underlying normal and abnormal brain function. However, translating results from rodents to humans is challenging, as ACC/OFC homologies between rodents and humans remain controversial. In contrast, human-nonhuman primate (NHP) ACC/OFC homologies are fairly well-established (5–7). Importantly, studies in NHPs and rats have demonstrated the topography of cortico-striatal anatomical projections (Table 1). Thus, NHPs provide a key intermediate step to delineate homologies central for linking rodent mechanistic studies to human pathologies.

The ACC regions include areas 25 (a25), 32 (a32), and 24 (a24) in NHPs and infralimbic (IL), prelimbic (PL), and cingulate (Cg) in rats. Although IL and a25 are largely seen as homologues and share emotion processing functions, PL and Cg homologies have generated significant controversy. These areas share certain functional features with the dorsolateral prefrontal cortex of NHPs (8, 9), but cytoarchitecture and connectivity point toward PL and Cg as homologous with a32 and a24 in primates, respectively (7, 10–12). Based on cytoarchitectonic similarity, the rat may possess regions homologous only to agranular NHP OFC (10). In contrast, based on thalamic projections, the entire primate OFC may be encapsulated within the rat lateral OFC (13).

In this paper, we used a striatal-centric approach to examine network homologies. We started with three well-conserved and well-defined structures: the shell of the nucleus accumbens (NAccS), the hippocampus, and the amygdala. The location, histochemistry, connections, and functions of the NAccS, hippocampus, and amygdala are similar across rodents and NHPs (14–22). Importantly, these structures are central to emotion processing (23–25). Within the ventral striatum, the NAccS is uniquely histochemically identifiable (26), and has distinct hypothalamic and extended amygdala projections (27). Likewise, the projections from the amygdala and the hippocampus to the striatum are consistent and reliable across species (20, 28–31). Thus, we focused first on frontal connectivity with the NAccS, the hippocampal-striatal projection zone, and the amygdala-striatal projection zone, which, together, we refer to as the striatal emotion processing network (EPN). In contrast to these well-defined areas, the nucleus accumbens “core” describes the area outside of the shell (26, 27). However, the lateral and dorsal boundary of the core is ambiguous, from both histochemical and connectivity perspectives (27, 32), and it merges imperceptibly into the

dorsal striatum. Thus, the lack of a precise dorsolateral boundary made a cross-species analysis of the core difficult.

In both NHPs and rodents, parts of the ACC/OFC project to the striatal EPN to varying degrees (33–37). We find that IL in rats and a25 in NHPs are the primary source of cortical input to the striatal EPN. Projections from other ACC/OFC areas overlap less with the EPN, but do overlap with IL/a25 terminal fields that are outside the EPN. We propose that the degree of overlap between these areas with the striatal EPN and IL/a25 indicates the extent to which they functionally interact with the EPN system. This provides critical data to the question of homologies, allowing us to improve on cross-species inferences about ACC/OFC-striatal networks.

Methods and Materials

Overview

Starting with a sizable database of cortico-striatal, hippocampal-striatal, and amygdala-striatal connectivities from our collections in the NHP (*Macaca fascicularis/mulatta/nemestrina*) and rat (*Rattus norvegicus*; Sprague-Dawley, Wistar, hooded strains), we selected cases based on good tracer transport and lack of contamination (Figure 1) (29, 31, 33–36, 38, 39). To ensure there were no gaps in areas of interest, we supplemented with new cases from our own collections and the literature. The connectivity overlap between each region of the ACC/OFC and the striatal EPN was compared between NHPs and rats to identify the locations of and relationships among ACC/OFC cortico-striatal terminal fields. Based on these analyses, we established similarities between specific ACC/OFC regions across species and segmented the striatum accordingly.

Data collection

Using material from the Haber, Groenewegen, and Deniau labs' histologically processed collections, we outlined injection sites and dense striatal terminal fields using Neurolucida software (MBF Bioscience) (35, 36). Dense striatal terminal fields were those that could be visualized at low magnifications (1.6 or 2.5X). Injection sites and terminal fields were modeled in 3D space using IMOD software (Boulder Laboratory for 3D Electron Microscopy) for visualization and analysis purposes (35, 36, 40, 41). Thus, data from each case was imported into the appropriate brain section using landmarks of key internal structures.

Cases drawn from the literature were from adult animals, with well-confined injection sites without white matter contamination, and where figures included the original charts of anterograde striatal labeling and photomicrographs or diagrams of the injection site. The locations of dense striatal terminal fields were determined using provided figures and textual descriptions, then incorporated on the appropriate section in the reference model. For full methods from cases in the literature, see corresponding papers (Table 1).

Analyses

We defined the striatal EPN as the area containing the NAccS, the hippocampal-striatal projection, and the amygdala-striatal projection. These were chosen because they are conserved across species, are related to emotional functions, and have easily identifiable locations and boundaries. We selected three matched reference coronal striatal sections at these levels: the rostral pole of the caudate; the mid-level of the NAccS; the decussation of the anterior commissure (Figure 2). Although projections of interest can be found caudal to this point, we limited our analyses to the rostral striatum, because the striatal EPN is best defined there and PFC-striatal projections are densest. Next, we transferred the dense striatal terminal fields for each case to fit the reference slices (35, 36), resulting in combined cortico-, amygdala-, and hippocampal-striatal maps from multiple sources, at corresponding levels in the two species. Analyses were designed to leverage PFC connectivity with the most conserved features of the striatum (EPN) to make inferences about ACC/OFC homologies (I–III). Identified homologies were used to segment the striatum according to its inputs (IV).

I. ACC/OFC overlap with the striatal EPN—The location and size of the NAccS within the central reference slice (Figure 2C) were identified for each species based on dense GluR1, 5-HT, and acetylcholinesterase staining and lack of calbindin staining (17, 42–45). We calculated the percent of each cortical case's striatal terminal field that was inside the NAccS, and created a 3D heat map of cortical injection sites based on this proportion. We did a similar analysis with the cortical inputs to the hippocampal and amygdala projection zones in this level of the striatum. Together, connectivities with the NAccS and hippocampal and amygdala projection zones indicated the extent of interaction between ACC/OFC areas and the striatal EPN.

II. Overlap between ACC/OFC projections with those from IL/a25—Because IL/a25 projections occupied the largest proportion of the striatal EPN, we assessed overlap between ACC/OFC terminal fields with those from IL/a25. We asked whether cortical location could predict terminal field position, and thus the extent of striatal projection overlap with the striatal EPN and the IL/a25 projection zone. We determined the average medial-lateral/dorsal-ventral (M-L/D-V) position of the cortical cases projecting to each location in the striatum, and created corresponding heat maps of the striatum. Warmer colors correspond to more medial and ventral frontal cortical inputs. These are closer to the EPN and the IL/a25 projection zone. We also determined the relationship between location of the center of each injection site and the terminal overlap with the IL/a25 projection zone in the central reference slice. We used a Pearson's correlation between M-L/D-V cortical position (normalized by cortical size) and overlap with IL/a25 projection zone. This analysis included cases that spanned subregions in the medial PFC (mPFC) and OFC.

III. Profile of overlap with the striatal EPN and ACC/OFC projections—We assessed the projections from medial orbital (MO), ventral/lateral orbital (VOLO), IL, PL, and Cg1/2 (in rat) and medial OFC (mOFC), central/lateral OFC (clOFC), a25, a32, and a24 (in NHP) to determine the mean proportion of overlap between striatal terminal fields from these ACC/OFC areas and with the striatal EPN (percentage of total striatal projection area

in the central slice falling within the NAccS or particular projection zones, averaged within cortical region). This created a cortico-striatal overlap profile (expressed as a pie chart) for each frontal area.

IV. Segmenting the striatum—Using the results from I–III, we segmented the striatum according to the relationship between projections from each ACC/OFC area and the striatal EPN.

Results

Overview

The location and proportion of the striatum occupied by the striatal EPN is similar across species (Figure 3). The NAccS is in a ventral position and occupies a similar proportion of striatal area in rats and NHPs (central reference slice: 10.5% rats, 10.4% NHPs). Similarly, the hippocampal and amygdala projection zones are of comparable sizes and positions within the ventral striatum of both species (hippocampus: 4.6% rat, 3.5% NHP; amygdala: 25% rat, 17.2% NHP). IL/a25 terminal fields had the greatest overlap with the EPN. Across species, specific ACC and OFC regions overlapped similarly with IL/a25 and the striatal EPN. Rat MO and PL and NHP mOFC and a32 share similar projections to the medial caudate. Rat VOLO and NHP clOFC have extensive central striatal projections. Rat Cg projections are mostly dorsal to the striatal EPN, while NHP a24 projects both ventrally and dorsally.

I. ACC/OFC overlap with the striatal EPN—One particular area in each species, IL in rat and a25 in NHP (5, 46), projects most strongly to the NAccS. On average, 52.9% of the IL-striatal projection zone and 50.0% of the NHP a25-striatal projection zone are within the NAccS (Figure 4A). While other areas in each species also project to the NAccS, their projection to this structure is more limited (Figure 4B). In rats, 10% of the PL projection, 0% of the Cg projection, and 1.4% of the OFC projection overlap the NAccS. In NHPs, 13.3% of the a32-striatal projection, 5.5% of the a24 projection, and 3.3% of the OFC projection overlap the NAccS. Similarly, IL/a25 terminal fields overlap considerably with the hippocampal-striatal projection zone, which is confined to the medial NAccS in the central striatal reference slice (Figure 5).

The frontal cases with the largest overlap with the amygdala-striatal projection zone are those with injection sites in IL/a25 (Figure 6A). On average, 96% of the IL-striatal projection and 76.8% of the a25-striatal projection are located within the amygdala projection area. Although other areas terminate here, none does so as strongly as cases centered in IL/a25 (Figure 6B). In rats, 28.7% of the PL projection, 1.8% of the Cg projection, and 10.6% of the OFC striatal projection fall within the amygdala projection zone. In NHPs, 19.4% of the a32-striatal projection, 11.5% of the a24 projection, and 12.6% of the OFC projection fall within the amygdala projection zone. In summary, IL/a25 have maximal overlap with the striatal EPN, and display similar projection patterns across rats and NHPs.

II. Overlap between ACC/OFC projections with those from IL/a25—There is a clear topography in the average cortical dorsal-ventral position of the injection sites placed along the medial PFC (mPFC) projecting to each location in the striatum: ventral and medial parts of the striatum have relatively more ventral cortical afferents (Figure 7A). Thus, moving dorsally in the mPFC, there is a gradual shift to projecting to more dorsal and lateral parts of the striatum. This pattern is particularly prominent in the central coronal slice we analyzed, where the striatal EPN is best-defined, and terminal fields from different PFC regions are maximally segregated. There is also a clear topography in the average medial-lateral position of injection sites placed on the orbital surface projecting to each location in the striatum: the ventral and medial striatum have more medial PFC afferents (Figure 7B). Thus, moving laterally in the OFC, there is a gradual shift to projecting to more dorsal and lateral parts of the striatum.

Absolute position can give important clues about cortico-striatal topography; however, we were also interested in directly assessing overlap with IL/a25. Thus, we examined the extent of the striatal terminal field overlap with the IL/a25 projection zone according to cortical position. The proportion of the mPFC-striatal terminal field overlapping with the IL/a25-striatal terminal field decreases with more dorsal mPFC injection sites in both species. Pearson's correlations between the normalized distance for each injection from the ventral cortical edge and the proportion overlap by the corresponding striatal terminal field with the IL/a25-striatal projection zone, using the central slice only (because it reliably contains IL projections in both species), showed significant relationships, rat--$r=-0.73$, $p<0.002$; NHP--$r=-0.69$, $p<0.001$ (Figure 8A). These results show that, in both species, the ventral mPFC-striatal terminals display a greater proportion overlap with the IL/a25-striatal projection zone than dorsal mPFC-striatal terminals do.

The proportion of the OFC-striatal terminal field overlapping with the IL/a25-striatal projection also decreases with more lateral OFC injection sites in both species. Pearson's correlations between the normalized distance for each case from the cortical medial edge and the proportion overlap in the striatal projection with the IL/a25-striatal terminal field showed significant relationships, rat--$r=-0.67$, $p=0.02$; NHP--$r=-0.79$, $p<0.01$ (Figure 8B). Thus, medial OFC-striatal terminals display a greater proportion overlap with the IL/a25-striatal projection than lateral OFC-striatal terminals. In summary, the overlap with the IL/a25 projection decreases with distance from the ventromedial surface of the PFC.

III. Profile of overlap with the striatal EPN and ACC/OFC projections—Analyzing each ACC and OFC area individually showed specific between-species correspondences (Figure 9). As described above, IL/a25 terminal fields are limited in scope compared to those from other areas: they are restricted mainly to the striatal EPN. IL/a25 projections also overlap substantially with OFC terminals. PL (rat) and a32 (NHP) are also similar: they project to the medial wall of the caudate; they project to the EPN, but not as extensively as IL/a25; their projections overlap substantially with terminals from amygdala, OFC, and IL/a25.

Comparing rat Cg and NHP a24 projections is more complex. Striatal fields from the NHP a24 cover a large portion of the rostral striatum, whereas those from the rat area Cg are more

limited. A24, but not Cg, projections overlap with inputs from the striatal EPN and a25; both overlap substantially with OFC terminal fields. Thus, a24 and Cg have different patterns of striatal projections. Importantly, NHP a24 can be divided into functionally distinct rostral, middle, and caudal regions. We asked whether any of these had striatal terminal fields more closely aligned with those from rat Cg. While the rostral a24-striatal projection is widespread and has all of the features described above, caudal a24 terminal fields appear unique. Like Cg, they are mostly limited to the dorsal striatum (Figure 10). Projections from both rostral and caudal portions of rat area Cg are confined to the dorsal striatum, and thus do not show the same differentiation as NHP a24.

MO/mOFC terminal fields are located not only in the striatal EPN, but also at the medial edge of the dorsal caudate (Figure 9). They do not extend into the lateral striatum. Ventrally, MO/mOFC projections overlap considerably with terminal fields from IL/a25. In contrast, VOLO/clOFC terminal fields in both species cover a larger region of the rostral striatum. They overlap substantially with those from the amygdala, IL/a25, and MO/mOFC ventrally. However, they also extend outside these areas, reaching into dorsal and central parts of the striatum.

IV. Segmenting the striatum—ACC/OFC projections to the striatum (Figure 11) were used to segment the striatum into four functionally distinct zones (Figure 12). First, in rats, the medial striatal EPN receives most of its input from IL (red zone, Figure 12). Additional input is derived from MO and area PL, but not from Cg. In NHPs, the medial striatal EPN receives most of its input from a25, and less from mOFC, a32, and a24. Second, in rats, VOLO projections to the striatal EPN (yellow zone) extend laterally to the main IL projection area. Similarly, in NHPs, OFC and a24 projections are present lateral to a25 terminals. Third, the medial wall of the striatum receives a unique set of projections from MO/mOFC and PL/a32 (pink zone). VOLO/clOFC and a24 (but not Cg) also project to this medial strip, but less exclusively. Finally, inputs to dorsal and lateral parts of the striatum are limited to Cg, a24, and VOLO/clOFC (blue zone).

Caudally, in both species, ACC/OFC terminals appear to occupy relatively less surface area, likely due to the presence of premotor and motor inputs. Similar to the more rostral section, at this caudal coronal level, the medial wall of the caudate receives a unique set of inputs from MO/mOFC and PL/a32. NHP a24 and rat VOLO/clOFC also project to this medial strip. VOLO inputs extend more dorsally in rats than clOFC inputs do in NHPs.

At the rostral striatal level, IL/a25 projections are very limited and isolated to the ventromedial striatum. Projections from other frontal cortical regions in both species appear less restricted and topographic than in the middle and caudal sections. For example, PL and rostral a24 projections span the entire medial-lateral width of the striatum at this level, unlike caudally. Although not analyzed here, the hippocampal-striatal projection is also more extensive at this rostralmost level (20, 31).

Discussion

In this study, we used projections to the NAccS and the hippocampal- and amygdala-striatal projection zones (together, the striatal EPN) to assess ACC/OFC homologies across rats and NHPs. First, we used connectivity with these conserved striatal features to establish that IL (rat) and a25 (NHP) are likely homologues. Although projections from other ACC/OFC areas overlap less with the striatal EPN, they do overlap with IL/a25 projections. Thus, we next determined the overlap between different ACC/OFC-striatal terminal fields and the IL/a25 projection zone, as a second measure of these areas' influence over basic emotional processes in the striatum. We found that both the mPFC and OFC of rats and NHPs obey similar organizational principles in their striatal projections. More dorsal and lateral ACC/OFC areas are less integrated with the EPN and IL/a25. These analyses suggest that the rat homologues of NHP a32, mOFC, and clOFC appear to be PL, MO, and VOLO, respectively. However, the rodent homologue of the primate rostral dorsal a24 is not clear, and may include portions of PL and Cg.

ACC/OFC homologies

IL cortex in rat and a25 in NHP are generally regarded as homologues. They are thought to play a central role in emotion processing (47), and have similar cytoarchitecture, location, and connections (7, 11, 48). IL and human a25 have also both been implicated in the successful retrieval of fear extinction memories (2). However, Kesner (9) suggests that IL, with PL and MO, is homologous to primate lateral PFC. Using circuit-based analyses, our data support the congruence between IL and a25. They both have a relatively limited striatal projection area, with terminals concentrated in the EPN.

Different authors consider PL to be homologous to NHP a32 (10, 48, 49), lateral PFC (9, 50), or a24 (51); the homologue of rodent Cg is similarly contentious (8, 10, 48). We find that a32 is most similar to PL, because of its medial projection and interface with the striatal EPN and IL/a25 (although parts of PL may also be homologous with portions of a24). Importantly, both PL and a32 projections are positioned at the intersection of the striatal EPN and IL/a25 projections on the one hand, and projections from more cognitive regions on the other. Finally, our analyses indicate that the rodent homologue of NHP a24 is not straightforward. Portions of PL may be equivalent to rostral a24 in NHP. Projections from Cg appear most similar to those from caudal a24, but may also have commonalities with rostral a24. Indeed, the fear learning literature points to a shared role for PL and a24 in the expression of conditioned fear (2), while a reward learning context suggests that PL and a32 guide outcome-directed behavior (48).

The homologies between rodent and primate OFC have important implications for how rodent OFC results ought to be translated. Passingham and Wise (10, 48) argue that granular OFC areas of the NHP (most of the orbital surface) have no homologue in the rodent. By contrast, others argue that the entire primate OFC may be homologous to the rat VOLO (13), because these regions share similar thalamic projections. Our results suggest that VOLO is homologous to NHP clOFC, with terminals spread throughout the central striatum. Functional studies concur: neurons in these areas both respond to sensory properties (see 7). By contrast, MO might best be compared to mOFC in NHPs. These areas are related to

motivational states and visceromotor context (7). Like those from PL, MO/mOFC terminal fields are positioned to interact with both the EPN and cognitive systems.

Implications for the study of psychiatric disorders

These results can facilitate cross-species research on psychiatric disorders. For example, activation of a25 and a32 is related to negative affect in MDD (52, 53) and drug-related cues in addiction (54, 55). Our results suggest that, particularly when studying cortico-basal ganglia networks, the mechanisms of such a25 and a32 abnormalities are most appropriately modeled in rodent IL and PL, respectively. Similarly, OCD, PTSD, and addicted patients show enhancements in a24 activity during symptom/craving provocation (2, 56–58); our results indicate that this region may have unique properties in primates relative to rodents. Finally, the mOFC is a critical area of disruption in OCD (59), an abnormality that has been successfully modeled in rodent MO (60).

Segmenting the striatum and integrative hubs

Our maps use conserved structures to demonstrate shared cortico-striatal topography across species. First, IL/a25 inputs dominate the medial striatal EPN in both species, while the lateral EPN contains a more diverse set of inputs. Notably, in both species, hippocampal-striatal terminals are confined to the ventromedial region (at the level of the central reference slice), where they can interface with IL/25 projections (20, 30, 31). Second, PL/a32 and MO/mOFC inputs extend up the medial caudate: this subarea is an important component of the ventral striatum (32). Third, the dorsal and lateral striatum in both species contains inputs from VOLO/clOFC and Cg/a24. Finally, there is substantial overlap in functionally distinct cortico-striatal terminal fields. Many of the details of this overlap are shared between rats and NHPs, indicating that cortico-striatal integration is conserved.

The observed pattern of cortical projections suggests a ventromedial to dorsolateral gradient of limbic to cognitive and motor inputs in both species (32, 61). Many functional and pharmacological studies of the rodent striatum only distinguish dorsal versus ventral portions (e.g., 62, 63), and boundaries between these subregions are ambiguous. However, both cortical and subcortical inputs are organized in a rotated (ventromedial to dorsolateral) fashion. Thus, there is also considerable evidence for medial/lateral and rostral/caudal differentiation (64–69). For example, goal-directed versus habitual actions seem to differentially involve the dorsomedial and dorsolateral portions of the striatum, respectively (68, 70). Our maps link these results with specific striatal subterritories of ACC/OFC connectivity (Figures 9–12).

Striatal regions that combine projections from functionally distinct cortical regions (referred to as hubs) may be critical for information integration within the basal ganglia (33). Thus, while a small number of inputs may dominate a striatal segment, other projections are also present, such that within each segment exist hubs with different combinations of inputs (33). Hubs are likely to be embedded within the segments identified in Figure 12, and also present in other striatal areas. For example, in the rostralmost section (Figure 2B/F), ACC/OFC projections likely overlap substantially with the hippocampal projection (20, 31). In caudal striatum, projections from the amygdala can interface with limited ACC/OFC terminal

fields. Future work will be able to identify, more precisely, the location of specific hubs and the strength of inputs.

Conclusions

Macroscale neuroimaging techniques for assessing connectivity highlight homologies between humans and NHPs (6, 71). Here we demonstrate how we can use the precision of anatomy to identify homologies between primates and rodents. Combined, these studies allow us to make connectivity-based inferences about homologies from rodents to NHPs and, finally, to humans.

Acknowledgments

This work was supported by P50 MH086400, R01 MH045673, and P50 MH106435 to SNH; R37 MH058883 to GJQ; R36 MH105039 to JRR; and F32 MH103931 to SRH. We thank Anna Borkowska-Belanger and Julia Lehman for technical assistance, Robert P. Vertes for helpful interpretations of his anatomical data, Jean-Michel Deniau and Veronique Coizet for loaning tissue, and the authors of the published anatomical data used to conduct this study for their careful work.

References

1. Mayberg HS, Brannan SK, Mahurin RK, Jerabek PA, Brickman JS, Tekell JL, et al. Cingulate function in depression: a potential predictor of treatment response. Neuroreport. 1997; 8:1057–1061. [PubMed: 9141092]
2. Milad MR, Quirk GJ. Fear extinction as a model for translational neuroscience: ten years of progress. Annu Rev Psychol. 2012; 63:129–151. [PubMed: 22129456]
3. Volkow ND, Wang GJ, Fowler JS, Tomasi D, Telang F. Addiction: beyond dopamine reward circuitry. Proc Natl Acad Sci U S A. 2011; 108:15037–15042. [PubMed: 21402948]
4. Haber SN, Heilbronner SR. Translational research in OCD: circuitry and mechanisms. Neuropsychopharmacology. 2013; 38:252–253. [PubMed: 23147494]
5. Petrides, M., Pandya, DN. Comparative architectonic analysis of the human and macaque frontal cortex. In: Boller, F., Grafman, J., editors. Handbook of Neuropsychology. Amsterdam: Elsevier; 1994. p. 17-58.
6. Sallet J, Mars RB, Noonan MP, Neubert FX, Jbabdi S, O'Reilly JX, et al. The organization of dorsal frontal cortex in humans and macaques. J Neurosci. 2013; 33:12255–12274. [PubMed: 23884933]
7. Ongur D, Price JL. The organization of networks within the orbital and medial prefrontal cortex of rats, monkeys and humans. Cerebral Cortex. 2000; 10:206–219. [PubMed: 10731217]
8. Seamans JK, Lapish CC, Durstewitz D. Comparing the prefrontal cortex of rats and primates: insights from electrophysiology. Neurotox Res. 2008; 14:249–262. [PubMed: 19073430]
9. Kesner R. Subregional analysis of mnemonic functions of the prefrontal cortex in the rat. Psychobiology. 2000; 28:219–228.
10. Wise SP. Forward frontal fields: phylogeny and fundamental function. Trends Neurosci. 2008; 31:599–608. [PubMed: 18835649]
11. Price JL. Definition of the orbital cortex in relation to specific connections with limbic and visceral structures and other cortical regions. Ann N Y Acad Sci. 2007; 1121:54–71. [PubMed: 17698999]
12. Preuss TM. Do Rats Have Prefrontal Cortex? The Rose-Woolsey-Akert Program Reconsidered. Journal of Cognitive Neuroscience. 1995; 7:1–24. [PubMed: 23961750]
13. Schoenbaum G, Roesch MR, Stalnaker TA. Orbitofrontal cortex, decision-making and drug addiction. Trends Neurosci. 2006; 29:116–124. [PubMed: 16406092]
14. Kelley AE. Functional specificity of ventral striatal compartments in appetitive behaviors. Annals of the New York Academy of Sciences. 1999; 877:71–90. [PubMed: 10415644]

15. Corbit LH, Muir JL, Balleine BW. The role of the nucleus accumbens in instrumental conditioning: evidence of a functional dissociation between accumbens core and shell. Journal of Neuroscience. 2001; 21:3251–3260. [PubMed: 11312310]
16. Voorn P, Gerfen CR, Groenewegen HJ. Compartmental organization of the ventral striatum of the rat: Immunohistochemical distribution of enkephalin, substance P, dopamine, and calcium-binding protein. J Comp Neurol. 1989; 289:189–201. [PubMed: 2478598]
17. Meredith GE, Pattiselanno A, Groenewegen HJ, Haber SN. Shell and core in monkey and human nucleus accumbens identified with antibodies to calbindin-D28k. J Comp Neurol. 1996; 365:628–639. [PubMed: 8742307]
18. Everitt BJ, Cador M, Robbins TW. Interactions between the amygdala and ventral striatum in stimulus-reward associations: studies using a second-order schedule of sexual reinforcement. Neuroscience. 1989; 30(1):63–75. [PubMed: 2664555]
19. McDonald AJ. Topographical organization of amygdaloid projections to the caudatoputamen, nucleus accumbens, and related striatal-like areas of the rat brain. Neuroscience. 1991; 44(1):15–33. [PubMed: 1722890]
20. Friedman DP, Aggleton JP, Saunders RC. Comparison of hippocampal, amygdala, and perirhinal projections to the nucleus accumbens: combined anterograde and retrograde tracing study in the Macaque brain. J Comp Neurol. 2002; 450:345–365. [PubMed: 12209848]
21. Squire LR. Memory and the hippocampus: a synthesis from findings with rats, monkeys, and humans. Psychol Rev. 1992; 99:195–231. [PubMed: 1594723]
22. Insausti R. Comparative anatomy of the entorhinal cortex and hippocampus in mammals. Hippocampus. 1993; 3(Spec No):19–26. [PubMed: 8287096]
23. Goto Y, Grace AA. Limbic and cortical information processing in the nucleus accumbens. Trends Neurosci. 2008; 31:552–558. [PubMed: 18786735]
24. Phelps EL, Joseph. Contributions of the Amygdala to Emotion Processing: From Animal Models to Human Behavior. Neuron. 2005; 48:175–187. [PubMed: 16242399]
25. Phelps EA. Human emotion and memory: interactions of the amygdala and hippocampal complex. Curr Opin Neurobiol. 2004; 14:198–202. [PubMed: 15082325]
26. Zaborszky L, Alheid GF, Beinfeld MC, Eiden LE, Heimer L, Palkovits M. Cholecystokinin innervation of the ventral striatum: A morphological and radioimmunological study. Neuroscience. 1985; 14(2):427–453. [PubMed: 3887206]
27. Heimer L, Zahm DS, Churchill L, Kalivas PW, Wohltmann C. Specificity in the projection patterns of accumbal core and shell in the rat. Neuroscience. 1991; 41(1):89–125. [PubMed: 2057066]
28. Krettek JE, Price JL. Amygdaloid projections to subcortical structures within the basal forebrain and brainstem in the rat and cat. J Comp Neurol. 1978; 178:225–254. [PubMed: 627625]
29. Wright CI, Beijer AVJ, Groenewegen HJ. Basal amygdaloid complex afferents to the rat nucleus accumbens are compartmentally organized. J Neurosci. 1996; 16(5):1877–1893. [PubMed: 8774456]
30. Kelley AE, Domesick VB. The distribution of the projection from the hippocampal formation to the nucleus accumbens in the rat: An anterograde and retrograde-horseradish peroxidase study. Neuroscience. 1982; 7:2321–2336. [PubMed: 6817161]
31. Groenewegen HJ, Vermeulen-Van der Zee E, Te Kortschot A, Witter MP. Organization of the projections from the subiculum to the ventral striatum in the rat. A study using anterograde transport of *Phaseolus vulgaris*-leucoagglutinin. Neuroscience. 1987; 23:103–120. [PubMed: 3683859]
32. Haber SN, McFarland NR. The concept of the ventral striatum in nonhuman primates. Ann N Y Acad Sci. 1999; 877:33–48. [PubMed: 10415641]
33. Averbeck BB, Lehman J, Jacobson M, Haber SN. Estimates of projection overlap and zones of convergence within frontal-striatal circuits. J Neurosci. 2014; 34:9497–9505. [PubMed: 25031393]
34. Calzavara R, Mailly P, Haber SN. Relationship between the corticostriatal terminals from areas 9 and 46, and those from area 8A, dorsal and rostral premotor cortex and area 24c: an anatomical substrate for cognition to action. Eur J Neurosci. 2007; 26:2005–2024. [PubMed: 17892479]

35. Haber SN, Kim KS, Mailly P, Calzavara R. Reward-related cortical inputs define a large striatal region in primates that interface with associative cortical connections, providing a substrate for incentive-based learning. J Neurosci. 2006; 26:8368–8376. [PubMed: 16899732]
36. Mailly P, Aliane V, Groenewegen HJ, Haber SN, Deniau JM. The rat prefrontostriatal system analyzed in 3D: evidence for multiple interacting functional units. J Neurosci. 2013; 33:5718–5727. [PubMed: 23536085]
37. Yeterian EH, Van Hoesen GW. Cortico-striate projections in the rhesus monkey: the organization of certain cortico-caudate connections. Brain Res. 1978; 139:43–63. [PubMed: 413609]
38. Berendse HW, Galisde Graaf Y, Groenewegen HJ. Topographical organization and relationship with ventral striatal compartments of prefrontal corticostriatal projections in the rat. J Comp Neurol. 1992; 316:314–347. [PubMed: 1577988]
39. Schilman EA, Uylings HB, Galis-de Graaf Y, Joel D, Groenewegen HJ. The orbital cortex in rats topographically projects to central parts of the caudate-putamen complex. Neurosci Lett. 2008; 432:40–45. [PubMed: 18248891]
40. Mailly P, Haber SN, Groenewegen HJ, Deniau JM. A 3D multi-modal and multidimensional digital brain model as a framework for data sharing. J Neurosci Methods. 2010; 194:56–63. [PubMed: 20043949]
41. Kremer JR, Mastronarde DN, McIntosh JR. Computer visualization of three-dimensional image data using IMOD. J Struct Biol. 1996; 116:71–76. [PubMed: 8742726]
42. Jongen-Relo AL, Docter GJ, Jonker AJ, Vreugdenhil E, Groenewegen HJ, Voorn P. Differential effects of dopamine depletion on the binding and mRNA levels of dopamine receptors in the shell and core of the rat nucleus accumbens. Mol Brain Res. 1994; 25:333–343. [PubMed: 7808232]
43. Fudge JL, Haber SN. Bed nucleus of the stria terminalis and extended amygdala inputs to dopamine subpopulations in primates. Neuroscience. 2001; 104:807–827. [PubMed: 11440812]
44. Zahm DS, Brog JS. On the significance of subterritories in the “accumbens” part of the rat ventral striatum. Neuroscience. 1992; 50:751–767. [PubMed: 1448200]
45. Brown P, Molliver ME. Dual serotonin (5-HT) projections to the nucleus accumbens core and shell: relation of the 5-HT transporter to amphetamine-induced neurotoxicity. J Neurosci. 2000; 20:1952–1963. [PubMed: 10684896]
46. Paxinos, G., Watson, C. The rat brain in stereotactic coordinates. New York: Academic; 1986.
47. Quirk GJ, Beer JS. Prefrontal involvement in the regulation of emotion: convergence of rat and human studies. Curr Opin Neurobiol. 2006; 16:723–727. [PubMed: 17084617]
48. Passingham, REaW, Steven, P. The Neurobiology of the Prefrontal Cortex: Anatomy, Evolution, and the Origin of Insight. United Kingdom: Oxford University Press; 2012.
49. Uylings HB, van Eden CG. Qualitative and quantitative comparison of the prefrontal cortex in rat and in primates, including humans. Prog Brain Res. 1990; 85:31–62. [PubMed: 2094901]
50. Granon S, Poucet B. Involvement of the rat prefrontal cortexx in cognitive functions: A central role for the prelimbic area. Psychobiology. 2000; 28:229–237.
51. Milad MR, Quirk GJ, Pitman RK, Orr SP, Fischl B, Rauch SL. A role for the human dorsal anterior cingulate cortex in fear expression. Biol Psychiatry. 2007; 62:1191–1194. [PubMed: 17707349]
52. Mayberg HS, Liotti M, Brannan SK, McGinnis S, Mahurin RK, Jerabek PA, et al. Reciprocal limbic-cortical function and negative mood: converging PET findings in depression and normal sadness. American Journal of Psychiatry. 1999; 156:675–682. [PubMed: 10327898]
53. Koenigs M, Grafman J. The functional neuroanatomy of depression: distinct roles for ventromedial and dorsolateral prefrontal cortex. Behav Brain Res. 2009; 201:239–243. [PubMed: 19428640]
54. Goudriaan AE, De Ruiter MB, Van Den Brink W, Oosterlaan J, Veltman DJ. Brain activation patterns associated with cue reactivity and craving in abstinent problem gamblers, heavy smokers and healthy controls: an fMRI study. Addict Biol. 2010; 15:491–503. [PubMed: 20840335]
55. Seo D, Lacadie CM, Tuit K, Hong KI, Constable RT, Sinha R. Disrupted ventromedial prefrontal function, alcohol craving, and subsequent relapse risk. JAMA Psychiatry. 2013; 70:727–739. [PubMed: 23636842]
56. Nakao T, Nakagawa A, Yoshiura T, Nakatani E, Nabeyama M, Yoshizato C, et al. Brain activation of patients with obsessive-compulsive disorder during neuropsychological and symptom

provocation tasks before and after symptom improvement: a functional magnetic resonance imaging study. Biol Psychiatry. 2005; 57:901–910. [PubMed: 15820711]

57. Goldstein RZ, Volkow ND. Dysfunction of the prefrontal cortex in addiction: neuroimaging findings and clinical implications. Nat Rev Neurosci. 2011; 12:652–669. [PubMed: 22011681]
58. Pitman RK, Rasmusson AM, Koenen KC, Shin LM, Orr SP, Gilbertson MW, et al. Biological studies of post-traumatic stress disorder. Nat Rev Neurosci. 2012; 13:769–787. [PubMed: 23047775]
59. Harrison BJ, Soriano-Mas C, Pujol J, Ortiz H, Lopez-Sola M, Hernandez-Ribas R, et al. Altered corticostriatal functional connectivity in obsessive-compulsive disorder. Arch Gen Psychiatry. 2009; 66:1189–1200. [PubMed: 19884607]
60. Ahmari SE, Spellman T, Douglass NL, Kheirbek MA, Simpson HB, Deisseroth K, et al. Repeated cortico-striatal stimulation generates persistent OCD-like behavior. Science. 2013; 340:1234–1239. [PubMed: 23744948]
61. Voorn P, Vanderschuren LJ, Groenewegen HJ, Robbins TW, Pennartz CM. Putting a spin on the dorsal-ventral divide of the striatum. Trends Neurosci. 2004; 27:468–474. [PubMed: 15271494]
62. Belin D, Everitt BJ. Cocaine Seeking Habits Depend upon Dopamine-Dependent Serial Connectivity Linking the Ventral with the Dorsal Striatum. Neuron. 2008; 57:432–441. [PubMed: 18255035]
63. Kelley AE. Ventral striatal control of appetitive motivation: role in ingestive behavior and reward-related learning. Neurosci Biobehav Rev. 2004; 27:765–776. [PubMed: 15019426]
64. Featherstone RE, McDonald RJ. Dorsal striatum and stimulus-response learning: lesions of the dorsolateral, but not dorsomedial, striatum impair acquisition of a stimulus-response-based instrumental discrimination task, while sparing conditioned place preference learning. Neuroscience. 2004; 124:23–31. [PubMed: 14960336]
65. Thorn CA, Atallah H, Howe M, Graybiel AM. Differential dynamics of activity changes in dorsolateral and dorsomedial striatal loops during learning. Neuron. 2010; 66:781–795. [PubMed: 20547134]
66. Kim HF, Hikosaka O. Parallel basal ganglia circuits for voluntary and automatic behaviour to reach rewards. Brain. 2015; 138:1776–1800. [PubMed: 25981958]
67. Kim HF, Hikosaka O. Distinct basal ganglia circuits controlling behaviors guided by flexible and stable values. Neuron. 2013; 79:1001–1010. [PubMed: 23954031]
68. Yin HH, Ostlund SB, Knowlton BJ, Balleine BW. The role of the dorsomedial striatum in instrumental conditioning. Eur J Neurosci. 2005; 22:513–523. [PubMed: 16045504]
69. Porrino LJ, Lyons D, Smith HR, Daunais JB, Nader MA. Cocaine self-administration produces a progressive involvement of limbic, association, and sensorimotor striatal domains. J Neurosci. 2004; 24:3554–3562. [PubMed: 15071103]
70. Yin HH, Knowlton BJ, Balleine BW. Lesions of dorsolateral striatum preserve outcome expectancy but disrupt habit formation in instrumental learning. Eur J Neurosci. 2004; 19:181–189. [PubMed: 14750976]
71. Mars RB, Jbabdi S, Sallet J, O'Reilly JX, Croxson PL, Olivier E, et al. Diffusion-weighted imaging tractography-based parcellation of the human parietal cortex and comparison with human and macaque resting-state functional connectivity. J Neurosci. 2011; 31:4087–4100. [PubMed: 21411650]
72. Reep RL, Cheatwood JL, Corwin JV. The associative striatum: organization of cortical projections to the dorsocentral striatum in rats. J Comp Neurol. 2003; 467:271–292. [PubMed: 14608594]
73. Hurley KM, Herbert H, Moga MM, Saper CB. Efferent projections of the infralimbic cortex of the rat. J Comp Neurol. 1991; 308:249–276. [PubMed: 1716270]
74. Sesack SR, Deutch AY, Roth RH, Bunney BS. Topographical organization of the efferent projections of the medial prefrontal cortex in the rat: an anterograde tract-tracing study with Phaseolus vulgaris leucoagglutinin. Journal Of Comparative Neurology. 1989; 290:213–242. [PubMed: 2592611]
75. Zeng D, Stuesse SL. Morphological heterogeneity within the cingulate cortex in rat: a horseradish peroxidase transport study. Brain Res. 1991; 565:290–300. [PubMed: 1726843]

76. Hoover WB, Vertes RP. Projections of the medial orbital and ventral orbital cortex in the rat. J Comp Neurol. 2011; 519:3766–3801. [PubMed: 21800317]

77. Vertes RP. Differential projections of the infralimbic and prelimbic cortex in the rat. Synapse. 2004; 51:32–58. [PubMed: 14579424]

78. Cho YT, Ernst M, Fudge JL. Cortico-amygdala-striatal circuits are organized as hierarchical subsystems through the primate amygdala. J Neurosci. 2013; 33:14017–14030. [PubMed: 23986238]

79. Chiba T, Kayahara T, Nakano K. Efferent projections of infralimbic and prelimbic areas of the medial prefrontal cortex in the Japanese monkey, Macaca fuscata. Brain Res. 2001; 888:83–101. [PubMed: 11146055]

80. Ferry AT, Ongur D, An X, Price JL. Prefrontal cortical projections to the striatum in macaque monkeys: evidence for an organization related to prefrontal networks. Journal of Comparative Neurology. 2000; 425:447–470. [PubMed: 10972944]

81. Paxinos, G., Huang, XF., Toga, AW. The rhesus monkey in stereotaxic coordinates. San Diego: Academic Press; 2000.

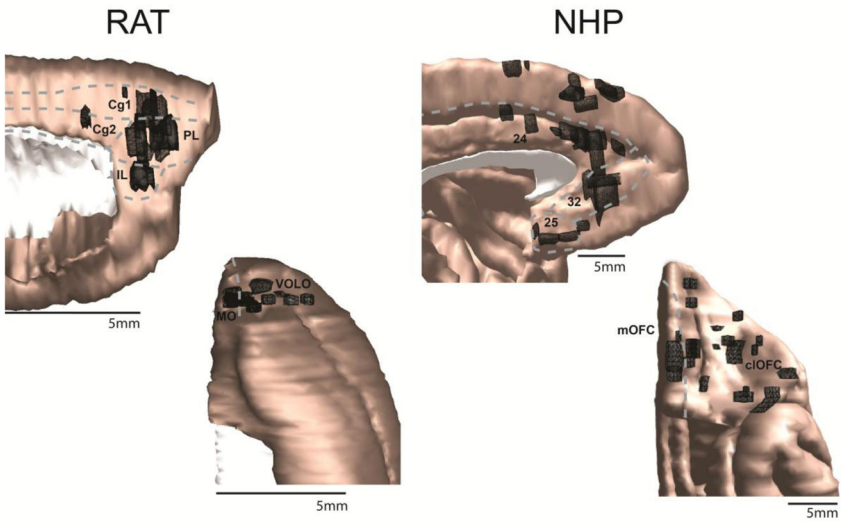

Figure 1. Injection sites

Injection sites for the rat (left) and NHP (right) are shown in black on the medial (top) and orbital (middle) frontal cortices. Approximate regional boundaries are demarcated with gray dotted lines. As in all figures, the rat brain has been enlarged relative to its actual size in comparison to the NHP brain for comparison purposes. clOFC=central/lateral orbitofrontal cortex; Cg1/2=cingulate areas 1/2; IL=infralimbic cortex; MO=medial orbital cortex; mOFC=medial orbitofrontal cortex; PL=prelimbic cortex; VOLO=ventral and lateral orbital cortex

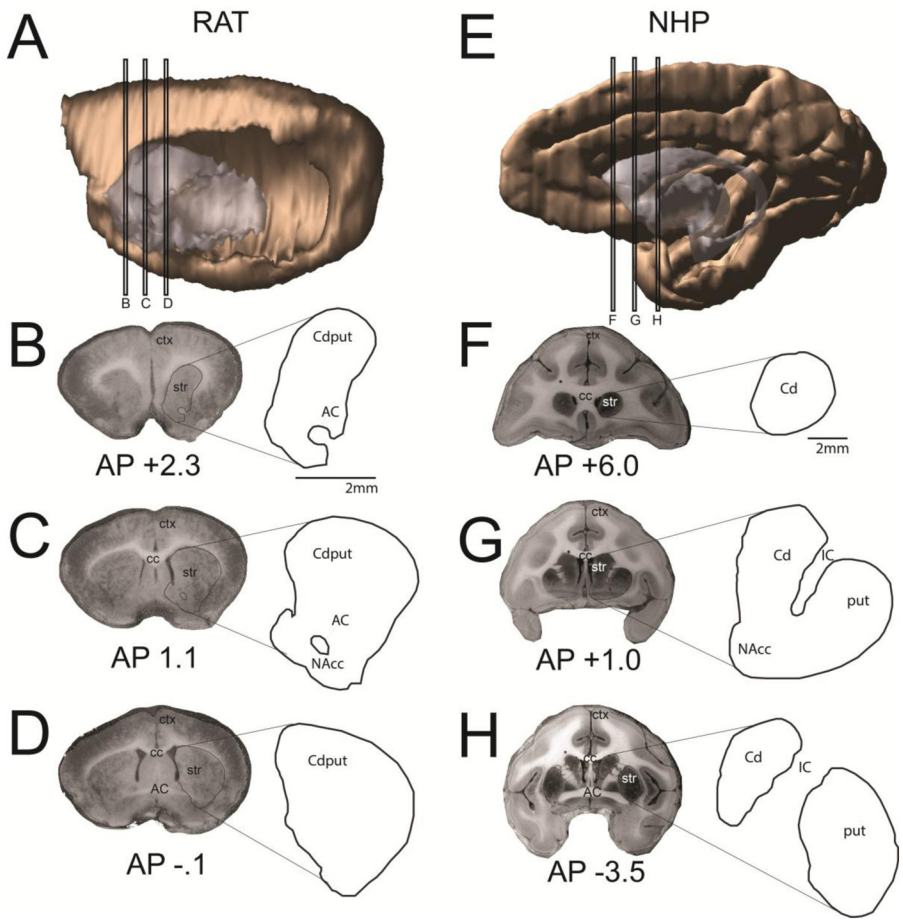

Figure 2. Striatal reference slices

A–D. Striatal reference slices for the rat A. Sagittal view showing levels from which coronal slices were drawn. B. Rostral striatal reference slice in the rat. C. Central striatal reference slice in the rat. D. Caudal striatal reference slice in the rat. E–H. Striatal reference slices for the NHP E. Sagittal view showing levels from which coronal slices were drawn. F. Rostral striatal reference slice in the NHP. G. Central striatal reference slice in the NHP. H. Caudal striatal reference slice in the NHP. AP=anterior-posterior distance from bregma, estimated from (46, 81); AC=anterior commissure; cc=corpus callosum; Cd=caudate; ctx=cortex; IC=internal capsule; NAcc=nucleus accumbens; put=putamen; str=striatum

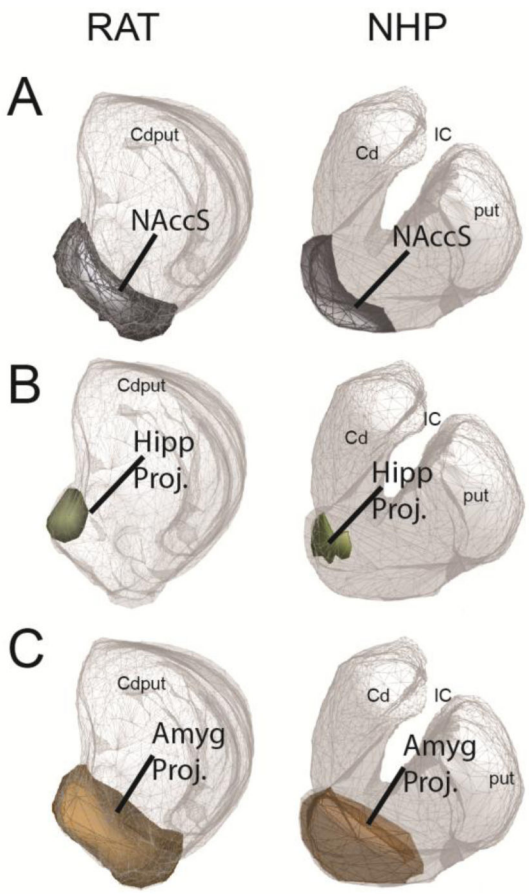

Figure 3. The striatal EPN in rats (left) and NHPs (right)

A. The NAccS is shown in gray on the central striatal reference slice. It occupies similar positions (ventral) and areas (10.5% in rats and 10.4% in NHPs) in both species. B. The hippocampal projection zone is shown in olive on the central striatal reference slice. It occupies similar positions (medial NAccS) and areas in both species (4.6% in rats and 3.5% in NHPs). C. The amygdala projection zone is shown in brown on the central striatal reference slice. It occupies similar positions (ventral, but extending dorsally to the NAccS) and areas (25% in rats and 17.2% in NHPs) in both species.

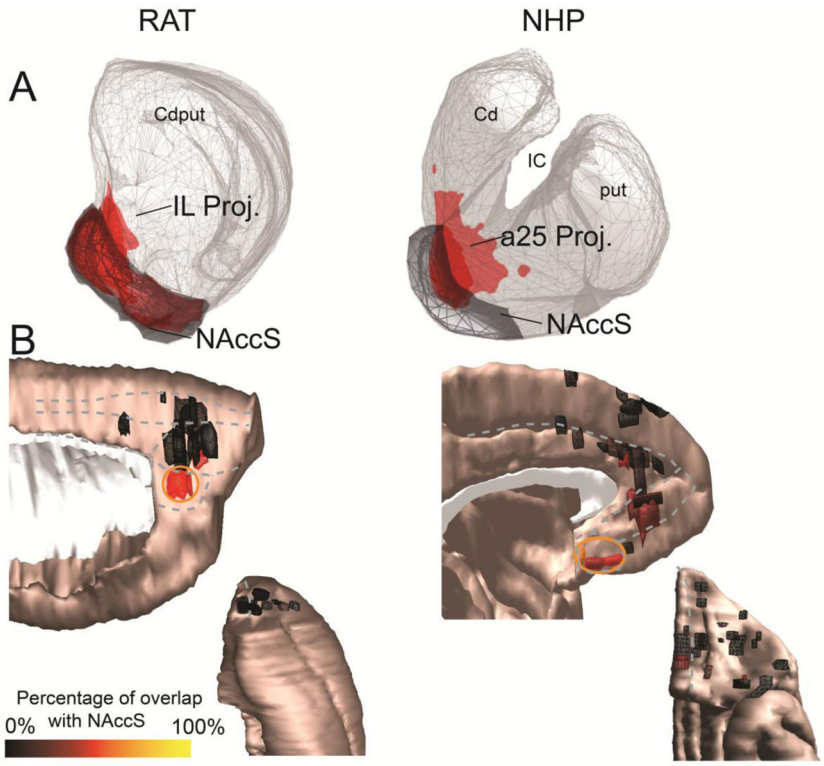

Figure 4. Projections to the shell of the nucleus accumbens from ACC and OFC regions

A. The cortico-striatal projections from the IL (rat, left) and a25 (NHP, right) show substantial overlap with the NAccS (gray) in both species. B. Medial sagittal (top) and orbital (bottom) views of cortical injection sites, colored according to the proportion of the corresponding striatal terminal field that occupies the NAccS. Warmer colors indicate greater overlap with the NAccS. Clear “hot spots” of cortico-striatal connectivity with the NAccS (orange circle) can be observed in the IL cortex (rat, left) and area 25 (NHP, right).

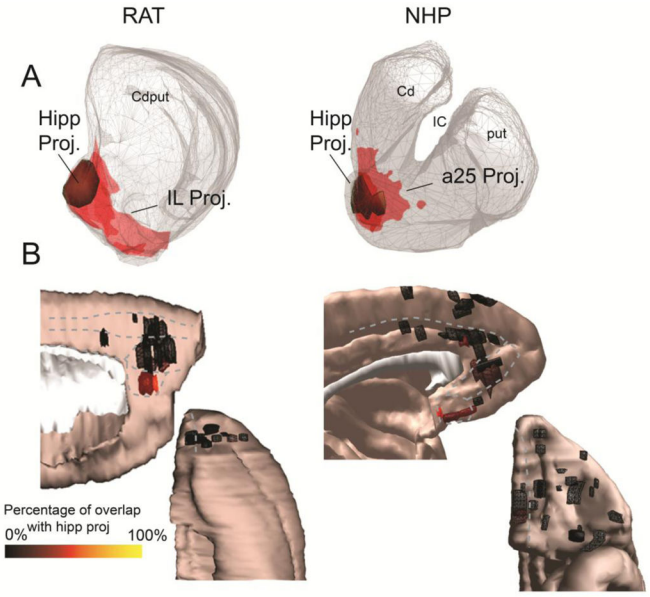

Figure 5. Projections to the hippocampal projection zone from ACC and OFC regions

A. The cortico-striatal projections from the IL (rat, left) and a25 (NHP, right) show substantial overlap with the hippocampal projection zone (olive) in both species. B. Medial sagittal (top) and orbital (bottom) views of cortical injection sites, colored according to the proportion of the corresponding striatal terminal field that occupies the hippocampal projection zone. Warmer colors indicate greater overlap with the hippocampal projection zone. Clear “hot spots” of cortico-striatal connectivity with the hippocampal projection zone can be observed in the IL cortex (rat, left) and area 25 (NHP, right).

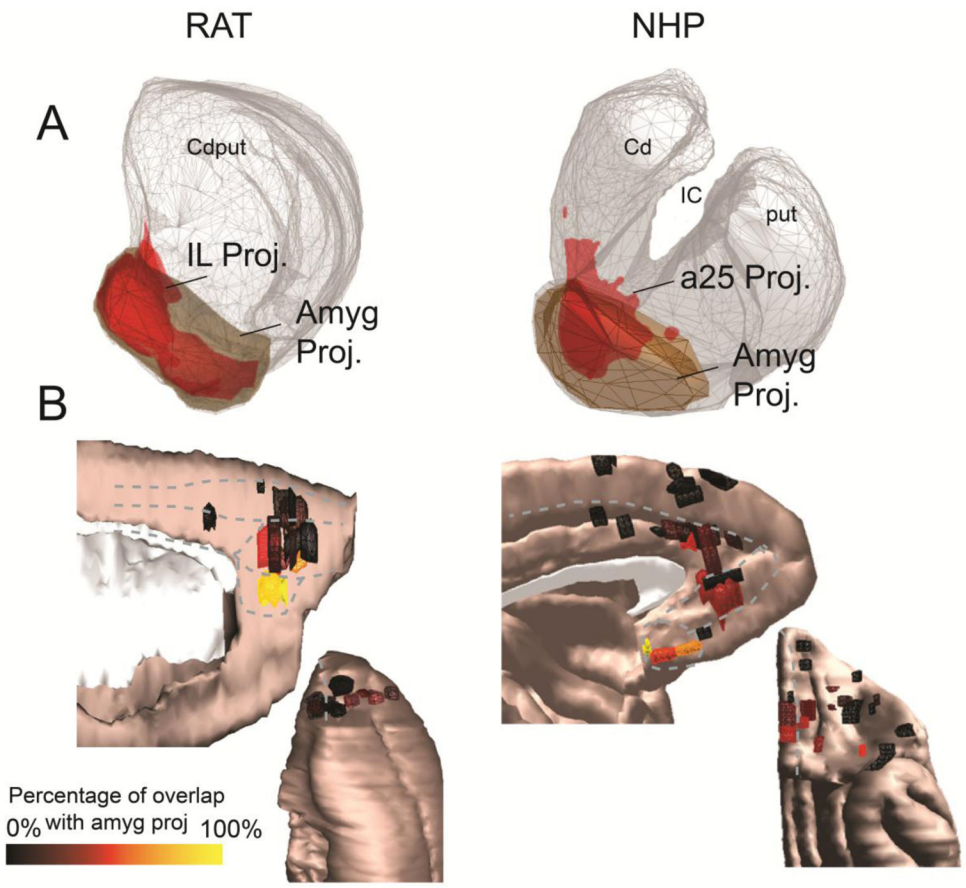

Figure 6. Projections to the amgydala projection zone from ACC and OFC regions

A. The cortico-striatal projections from the IL (rat, left) and a25 (NHP, right) show substantial overlap with the amygdala-striatal projection region (brown) in both species. B. Medial sagittal (top) and orbital (bottom) views of cortical injection sites, colored according to the proportion of the corresponding striatal terminal field that occupies the amygdala projection zone. Warmer colors indicate greater overlap with the amygdala projection zone. Clear “hot spots” of cortico-striatal connectivity with the amygdala projection zone can be observed in the IL cortex (rat, left) and a25 (NHP, right).

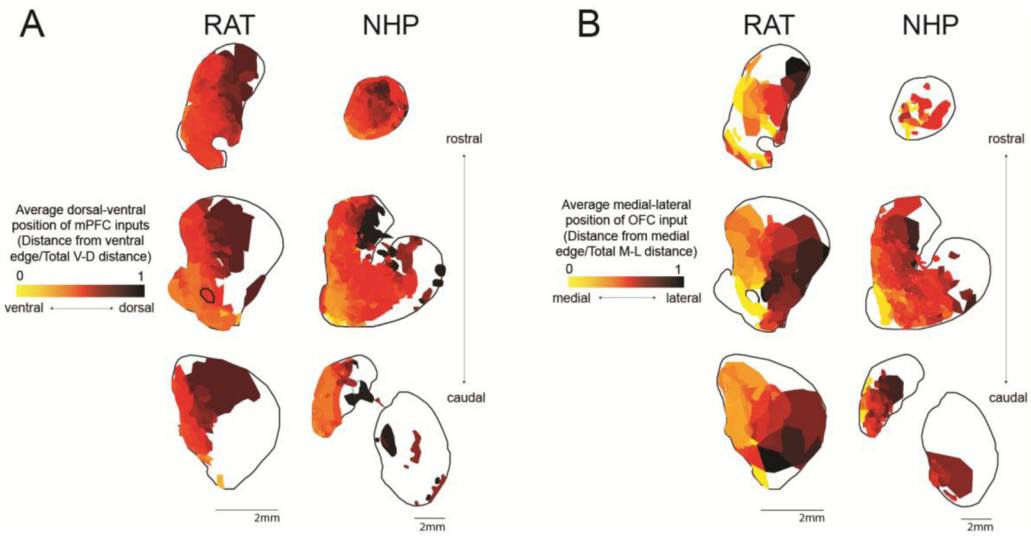

Figure 7. Striatal projection location is related to cortical position in both species

A. Heat maps show the average ventral-dorsal position of mPFC input to each position in the striatum, at 3 rostral-caudal levels (as shown in Figure 2). Maps were created by averaging the V-D position of every mPFC injection site that resulted in dense terminal field in the specified striatal location. V-D positions were normalized according to the total V-D distance on the medial surface at the coronal slice corresponding to the center of the injection site in question. B. Heat maps show the average medial-lateral position of OFC input to each position in the striatum, at 3 rostral-caudal levels (as shown in Figure 1). Maps were created by averaging the M-L position of every OFC injection site that resulted in dense terminal field in the specified striatal location. M-L positions were normalized according to the total M-L distance on the orbital surface at the coronal slice corresponding to the center of the injection site in question.

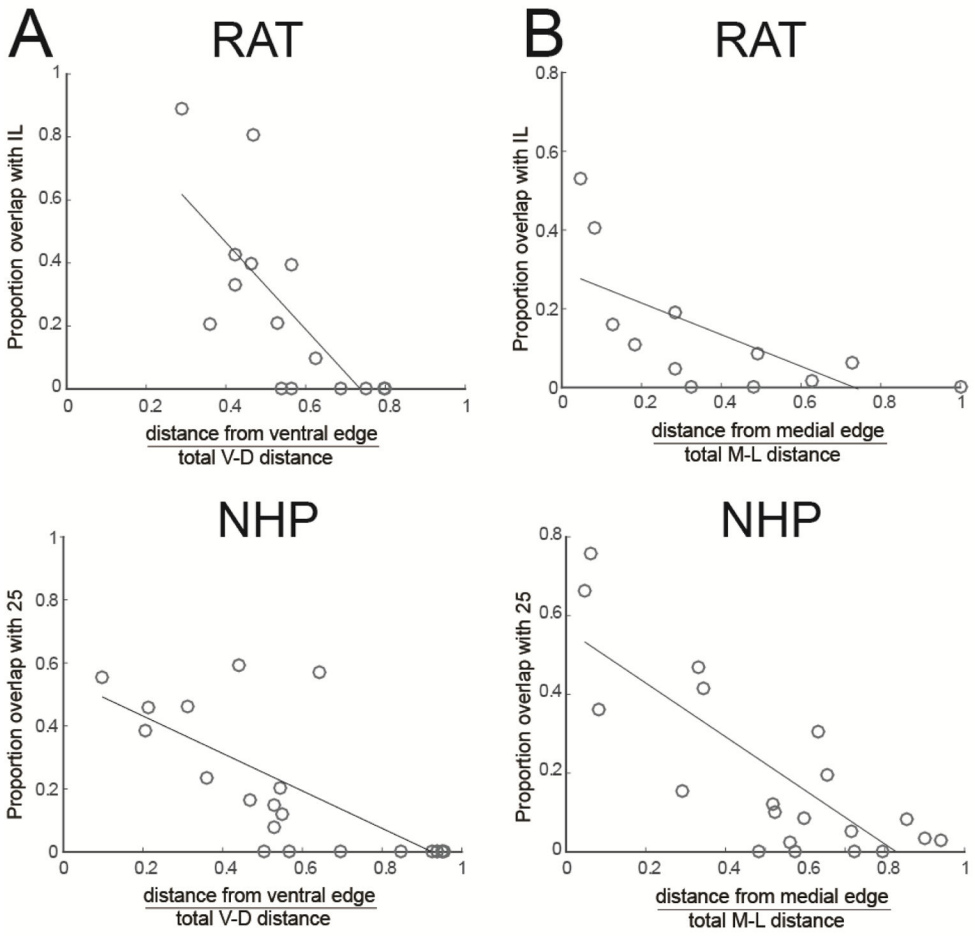

Figure 8. Comparable mPFC and OFC-striatal organization across species

A. Proportion of mPFC striatal field overlap (central slice as shown in Figures 2C and 2G) with IL/a25 projection zone decreases with more dorsal injection sites in rats (top) and NHPs (bottom). B. Proportion of OFC striatal field overlap (central slice as shown in Figures 2C/G) with IL/a25 projection zone decreases with more lateral injection sites in rats (top) and NHPs (bottom). Thus, more lateral and dorsal ACC/OFC areas are less integrated with the striatal EPN.

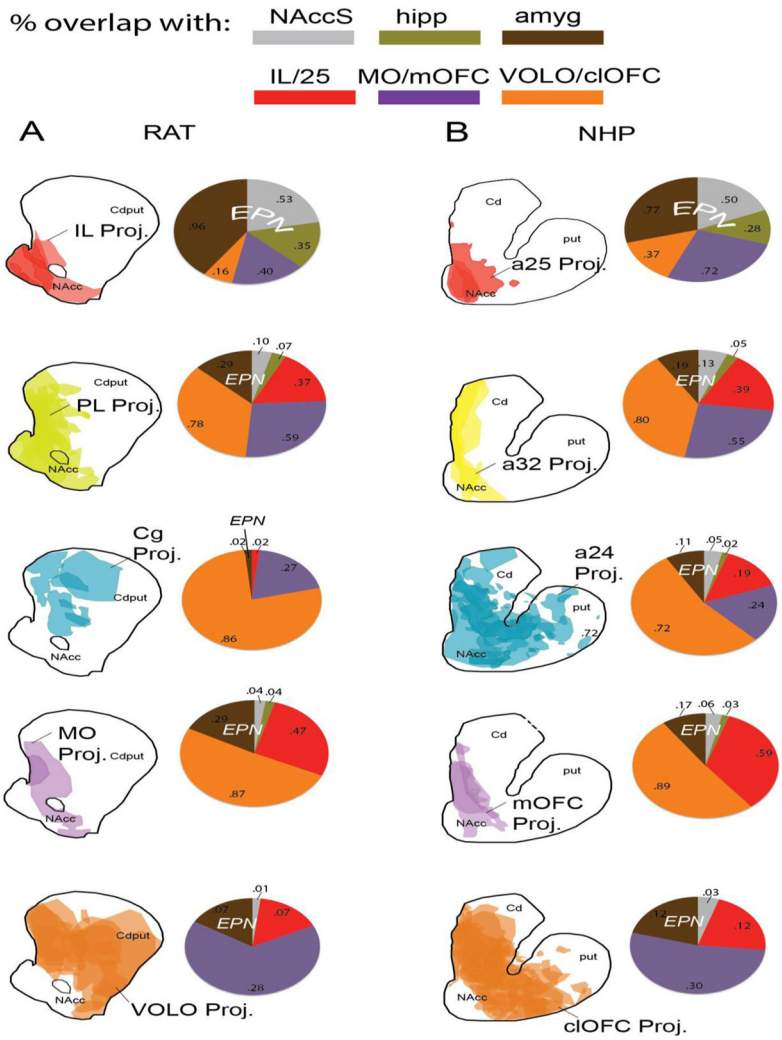

Figure 9. Detailed analyses of individual ACC and OFC areas

A–B: Drawings show the overlapping striatal terminal fields from different frontal cortical cases, grouped by region. Pie charts show proportion of the corresponding striatal terminal field that overlaps with projection zones from the IL/a25 (red), MO/mOFC (purple), VOLO/clOFC (orange), amygdala (brown), and hippocampus (olive), and the NAccS (gray). Numbers inside pie charts indicate the mean proportion of the cortical area's striatal terminal field overlapping with the striatal zone indicated (central coronal slice, Figure 2C/G). For example, for the pie chart shown at the upper left, the 96% of the average terminal field from IL falls within the amygdala-striatal projection zone, 53% falls within the NAccS, 35% falls within the hippocampal-striatal projection zone, 40% falls within the MO-striatal projection zone, and 16% falls within the VOLO-striatal projection zone.

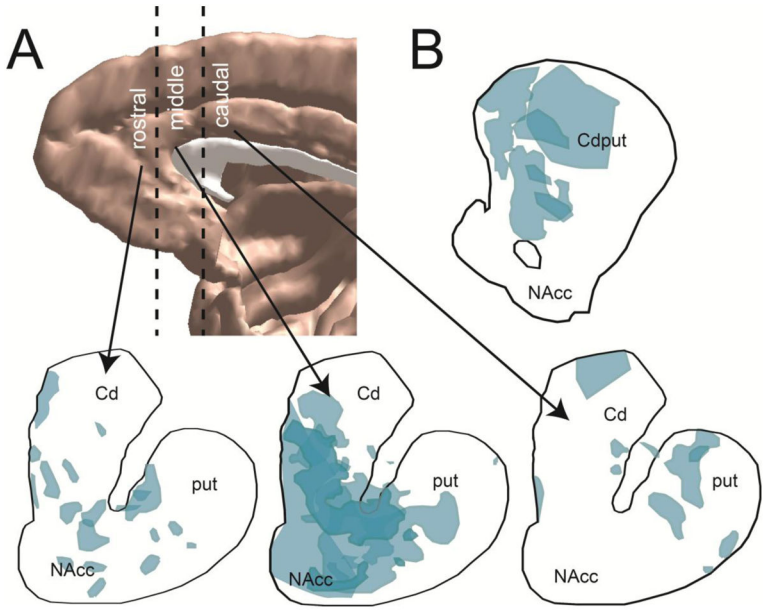

Figure 10. Rostral vs caudal primate a24 show different striatal projection patterns

A. Upper left shows subdivsions of rostral, middle, and caudal dACC zones in NHP (boundaries indicated by dotted lines). Bottom shows corresponding striatal projections. Rostral and middle a24 terminals span ventral and dorsal striatum (and elsewhere in the paper are combined and described as only “rostral a24”). Caudal primate a24 terminals are mainly located in the dorsal striatum. B. a24 subdivisions used for A. C. The rat Cg striatal projection is shown for comparison purposes (there are no rostral-caudal differences in rat Cg projections).

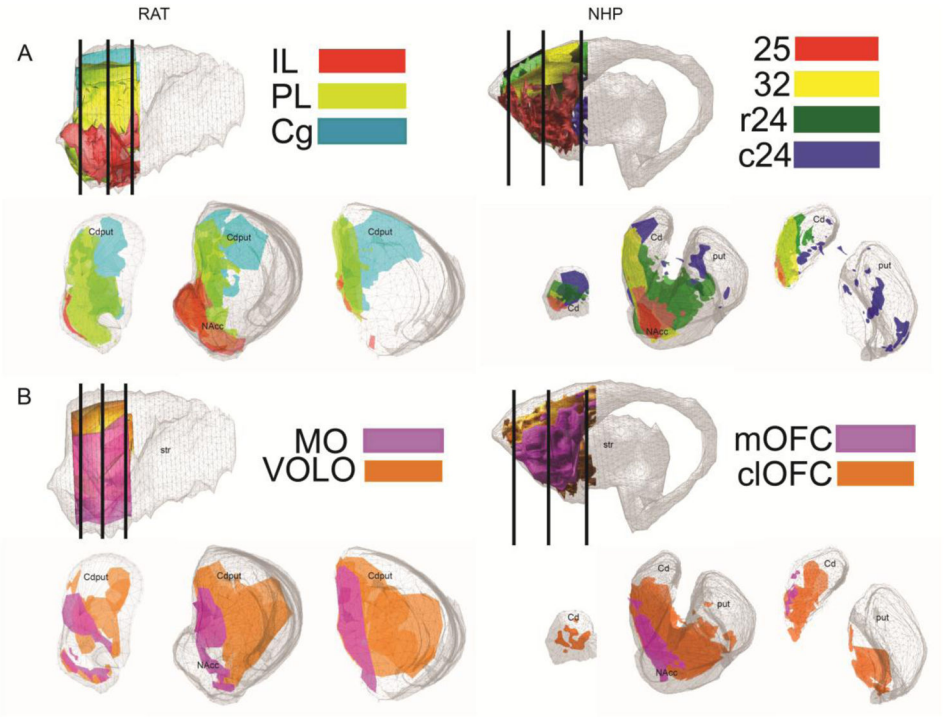

Figure 11. Striatal projection zones according to identifiable ACC/OFC homologies

A. IL (red), PL (yellow-green), and Cg (teal) projections in rat (left); areas a25 (red), a32 (yellow), rostral 24 (r24, green), and caudal a24 (c24, blue) in NHP (right). B. MO/mOFC (purple) and VOLO/clOFC (orange) projections in rat (left) and NHP (right). For both species, reference slice locations are shown in sagittal slices at upper left, and in Figure 2.

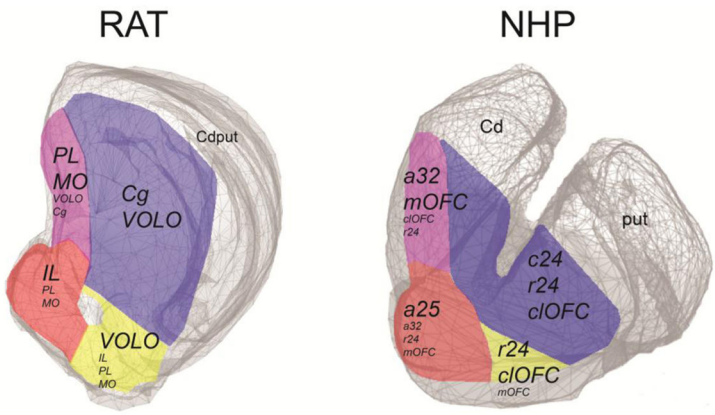

Figure 12. Schematic representation of cross-species striatal segmentation, according to characteristic ACC/OFC projections

Although there are substantial areas of overlap among cortical terminal fields, different striatal segments have unique combinations of ACC/OFC inputs (listed in italics within each segment; dominant ones are in larger font). Within each segment, hubs of unique cortical and subcortical connections can be found.

Table 1

Injection sites & sources.

RAT	**IL**	**PL**	**Cg**	**OFC**	**hipp**	**amyg**	**TOTALS**
Deniau collection		4	2	2			8
Groenewegen collection	2	1	2	7	2	5	19
Haber collection						1	1
Kelley & Domesick (30)					1		
Krettek & Price (28)						4	4
Reep et al. (72)				1			1
Hurley et al. (73)	1						1
Sesack et al. (74)		3	1				4
Zeng & Stuesse (75)		1					1
Vertes collection (76, 77)	1	1		2			4
TOTALS	4	10	5	12	3	10	54
NHP	vmPFC	OFC	dACC	dmPFC	hipp	amyg	TOTALS
Friedman et al. (20)					2	5	7
Cho et al. (78)						4	4
Haber collection	3	9	7	7	1	2	29
Chiba et al. (79)	2		1				3
Ferry et al. (80)	2	11	1				14
TOTALS	7	20	9	7	3	11	57